International Immunopharmacology 70 (2019) 147–155

Contents lists available at ScienceDirect

International Immunopharmacology

journal homepage: www.elsevier.com/locate/intimp

The selective NLRP3 inflammasome inhibitor MCC950 alleviates cholestatic liver injury and fibrosis in mice

Junwen Qu[1], Zhiqing Yuan[1], Guiyang Wang, Xiaopeng Wang, Kewei Li*

Department of Biliary- Pancreatic Surgery, Renji Hospital, School of Medicine, Shanghai Jiao Tong University, No. 160, Pujian Road, Pudong New Area, Shanghai 200127, China

A B S T R A C T

Cholestasis occurs in many clinical circumstances and leads to severe liver disorders. MCC950, a small-molecule NLRP3 inhibitor, was previously shown to have anti-inflammatory effects. However, these effects have not yet been examined in cholestatic liver injury. This study aimed to investigate the role of NLRP3 inflammasome and test the therapeutic efficacy and molecular mechanisms of MCC950 in cholestatic liver injury through the common bile duct ligation (BDL) model in mice. The influence of MCC950 on histological changes, levels of liver damage, neutrophil infiltration, liver cell death, inflammatory cytokine levels, and NLRP3 inflammasome expression were examined. The results of the current study confirmed that NLRP3 components were up-regulated during bile duct obstruction. MCC950 treatment significantly alleviated BDL-induced liver injury by reducing production of the pro-inflammatory cytokines IL-1β and IL-18 and inhibiting neutrophil infiltration and hepatic cell death. Moreover, MCC950 significantly inhibited NLRP3 activation during cholestatic liver injury. In addition, transcriptome analysis indicated that Toll-like receptor signaling may be involved in the protective effects of MCC950 in cholestatic liver injury. In conclusion, experimental findings demonstrate that MCC950 exerted protective effects in cholestatic liver injury and liver fibrosis by blocking NLRP3 inflammasome activation and the mechanism was partially attributed to inhibition of Toll-like receptor signaling. The present study indicates MCC950 could potentially be an effective therapeutic strategy for the treatment of cholestatic liver injury.

1. Introduction

Cholestasis is a common clinical syndrome characterized by an impairment of bile secretion and flow. This condition can result from diverse etiologies such as extrahepatic biliary obstruction by stones or tumors, biliary atresia, intrahepatic cholestasis by virus, drugs, alcohol, pregnancy, or autoimmune disorders. Accumulation of toxic bile acids in the liver can lead to severe liver damage, progressive liver fibrosis, and eventually cirrhosis and liver failure [1–3]. However, the primary trigger for liver injury induced by cholestasis is not clear, and effective prevention and treatment measures are still lacking.

The NOD-like receptor protein 3 (NLRP3), an intracellular multi-protein complex, the adaptor molecule apoptosis-associated speck-like protein (ASC), and the effector molecule pro-caspase-1 comprise the NLRP3 inflammasome. NLRP3 inflammasome activation can be induced by diverse stimuli including pathogen-associated molecular patterns (PAMPs), damage-associated molecular patterns (DAMP), crystals, particles, and reactive oxygen species (ROS) in both parenchymal and nonparenchymal cells. Upon stimulation, NLRP3 recruits pro-caspase-1 and the adaptor molecule ASC, resulting in activation of caspase-1. Thus, activated caspase-1 triggers the maturation and secretion of interleukin-1β (IL-1β) and interleukin-18 (IL-18), initiating inflammation. Recently, several studies have elucidated the pivotal role of NLRP3 inflammasome activation as a trigger in the development of a variety of liver diseases such as liver ischemia-reperfusion injury, acetaminophen-induced liver injury, alcoholic and non-alcoholic fatty liver diseases, non-alcoholic steatohepatitis (NASH), and biliary atresia [4–7]. Moreover, IL-1β has been elevated in cases of cholestatic liver injury in bile duct ligation in mice. It is an important mediator that recruits inflammatory cells into the hepatic tissue and promotes fibrogenesis. Therefore, these novel findings raise the possibility that modulation of inflammasome signaling in the liver can block the progression of hepatic inflammation and fibrosis.

MCC950 is a recently developed specific small molecule inhibitor that can selectively block NLRP3 inflammasome activation both in vitro and in vivo [8]. Previous studies have reported MCC950 reduced IL-1β production and attenuated the severity of experimental models of lung ischemia-reperfusion injury [9], ulcerative colitis [10], myocardial infarction [11], and liver transplantation [12]. Furthermore, a recent study suggested that MCC950 exerts protective effects for liver inflammation and fibrosis in two models of NASH [13]. However, the efficacy of MCC950 in cholestatic liver injury has not been discussed.

In this study, we aim to determine whether NLRP3 inflammasome activation contributes to cholestatic liver injury and fibrosis, and

* Corresponding author.
E-mail address: keweipig@126.com (K. Li).
[1] These authors contributed equally to this work.

https://doi.org/10.1016/j.intimp.2019.02.016
Received 6 November 2018; Received in revised form 12 January 2019; Accepted 10 February 2019
Available online 22 February 2019

investigate the therapeutic effects and exact underlying mechanisms of its selective inhibitor MCC950.

2. Materials and methods

2.1. Animals

Specific pathogen-free male C57BL/6 mice (6–8 weeks, 19–23 g) were purchased from Shanghai SLAC Laboratory Animal Co., Ltd. and maintained in the Department of Animal Experiments, Renji Hospital, Medical School of Shanghai, Jiao Tong University. Animal care and operations conformed to the guidelines of the National Institutes of Health for the care and use of laboratory animals (NIH Publications No. 8023, revised 1978) and approved by the Ethics Committee of Renji Hospital. Mice were randomly assigned to groups as follows: sham operation group (sham), BDL group (BDL), and BDL + MCC950 pretreatment group (BDL + MCC950). Bile duct ligation was performed according to the protocol in JOVE [14]. Briefly, mice were anesthetized with 4% Chloral hydrate (dissolved in saline, Sigma, St. Louis, MO, USA). Followed by midline abdominal incision, the common bile duct was exposed, doubly ligated with 4–0 silk sutures, and resected between the ligatures. Sham-operated group underwent the same procedure without bile duct ligation served as healthy controls. The BDL + MCC950 group was given MCC950 (Selleck, Houston, TX) 10 mg/kg body weight in 0.9% NaCl intraperitoneally every day, first injection was performed right after operation, while the mice in Sham group and BDL group were injected with an equal volume vehicle. After seven days, the mice were sacrificed after anesthesia. The serum and livers were harvested and stored at −80 °C.

2.2. Liver histology and immunohistochemistry

Liver tissues were fixed in 4.5% buffered formalin for at least 24 h and embedded in paraffin. Sections were stained with hematoxylin/eosin (H&E) and Sirius Red after deparaffinization and dehydration. Immunohistochemical staining was carried out by incubation of the sections with F4/80 (Biolegend, San Diego, CA, USA), myeloperoxidase (MPO), α-smooth muscle actin (α-SMA) and NLRP3 (Servicebio, Wuhan, China) antibody, then visualized by color development with diaminobenzidine.

2.3. Liver damage assessment

Serum alanine aminotransferase (ALT) and aspartate transaminase (AST) levels were measured using the commercially available assay kit purchased from Nanjing Jiancheng Bioengineering Institute (Nanjing, China) according to the manufacturer's instructions.

2.4. TUNEL assay

TUNEL assay was performed on liver paraffin-embedded tissue sections using a commercial kit (Roche, Basel, Switzerland) according to the manufacturer's instructions. Nuclei were stained with 4′, 6-diamidino-2-phenylindole (DAPI), and TUNEL positive cells were visualized with a fluorescence microscope (NIKON, Tokyo, Japan).

2.5. Serum cytokines analysis

The serum was collected and cytokine levels measured using an ELISA kit to determine the expression of IL-1β (Beyotime Institute of Biotechnology, Hangzhou, China) and IL-18 (Sino Biological Inc., Beijing, China) according to the manufacturer's instructions.

2.6. Real-time quantitative PCR

Total RNA was extracted from mouse liver tissue using TRIzol reagent (Sigma, St. Louis, MO, USA) and 1 μg total RNA was reverse-transcribed into cDNA using the PrimeScript RT Reagent Kit (Takara, Shiga, Japan). Real-time quantitative PCR was performed on an Applied Biosystems ViiA™ 7 Real-Time PCR System (Applied Biosystems, Foster City, CA, USA) using SYBR Premix Ex Taq (Takara, Code NO. RR82LR). The primers used are summarized in the Supplementary Table 1. Gene expression levels were evaluated and normalized to β-actin using the $2^{\Delta\Delta CT}$ method.

2.7. Western blot analysis

The liver tissue homogenates or cells were lysed in a cold RIPA buffer (Beyotime Institute of Biotechnology, Hangzhou, China) supplemented with a protease inhibitor cocktail at 1:100 for 20 min on ice. Protein concentrations were measured using a BCA protein assay (Yeasen Biotech Co., Ltd., Shanghai, China). Proteins were separated by electrophoresis with 10% or 12% SDS-PAGE gels and transferred to a PVDF membrane. The membranes were blocked using 5% skim milk for 1 h at room temperature. Next, the membranes were incubated at 4 °C overnight with antibodies including NLRP3, IL-1β (Cell Signaling Technology, Beverly, MA, USA), caspase-1 (Proteintech Group, Inc., Chicago, IL, USA), and anti-β-actin (Yeasen, Shanghai, China). The membranes were washed three times in TBST. The membranes were incubated with the appropriate secondary antibodies for 1 h at room temperature. The expression of targeted proteins was determined using a Bio-Rad ChemiDoc MP imaging system (Hercules, CA, USA). The β-actin levels were used as an internal control.

2.8. RNA-Seq and data analysis

Total RNA was isolated from the liver tissue using TRIzol® reagent (Invitrogen, Carlsbad, CA, USA) according the manufacturer's instructions, and RNA purity and integrity were assessed using the Nanodrop 2000 (Thermo Fisher Scientific, Waltham, MA, USA) and 2100 Bioanalyzer Instruments (Agilent, Santa Clara, CA, USA), respectively. The RNA-seq transcriptome library was prepared following the TruSeqTM RNA sample preparation Kit from Illumina (Illumina, San Diego, CA, USA) using 5 μg of total RNA. After library construction, a paired-end RNA-seq library was sequenced with the Illumina HiSeq 4000 (2 × 150 bp read length). The raw reads were trimmed and quality controlled by SeqPrep (https://github.com/jstjohn/SeqPrep) and Sickle (https://github.com/najoshi/sickle) with default parameters. Then, TopHat software [15] was used to map the cleaned reads to a murine reference genome. To identify differential expression genes (DEGs) between two different samples the expression level of each transcript was calculated according to the fragments per kilobase million (FPKM). DEGs with a log2 fold change > 1 and a P-value < 0.05 were analyzed to identify enriched biological processes. Gene ontology (GO) functional enrichment and Kyoto Encyclopedia of Genes and Genomes (KEGG) pathway analysis was performed with Metascape [16] and KOBAS [17]. Differential expressions of genes selected from each category were verified by RT-quantitative PCR (QRT-PCR). The list of primers is given in the Supplementary Table 1.

2.9. Statistical analysis

All data are indicated as the means ± SEM (standard error of the mean). The difference between two groups was determined using paired or unpaired Student's *t*-test. Survival curves were analyzed using the Kaplan-Meier method, and the difference was calculated using the log-tank test. Statistical analyses were conducted using GraphPad (Graph Pad Software Inc., CA, USA). Differences were considered to be significant at $p < 0.05$.

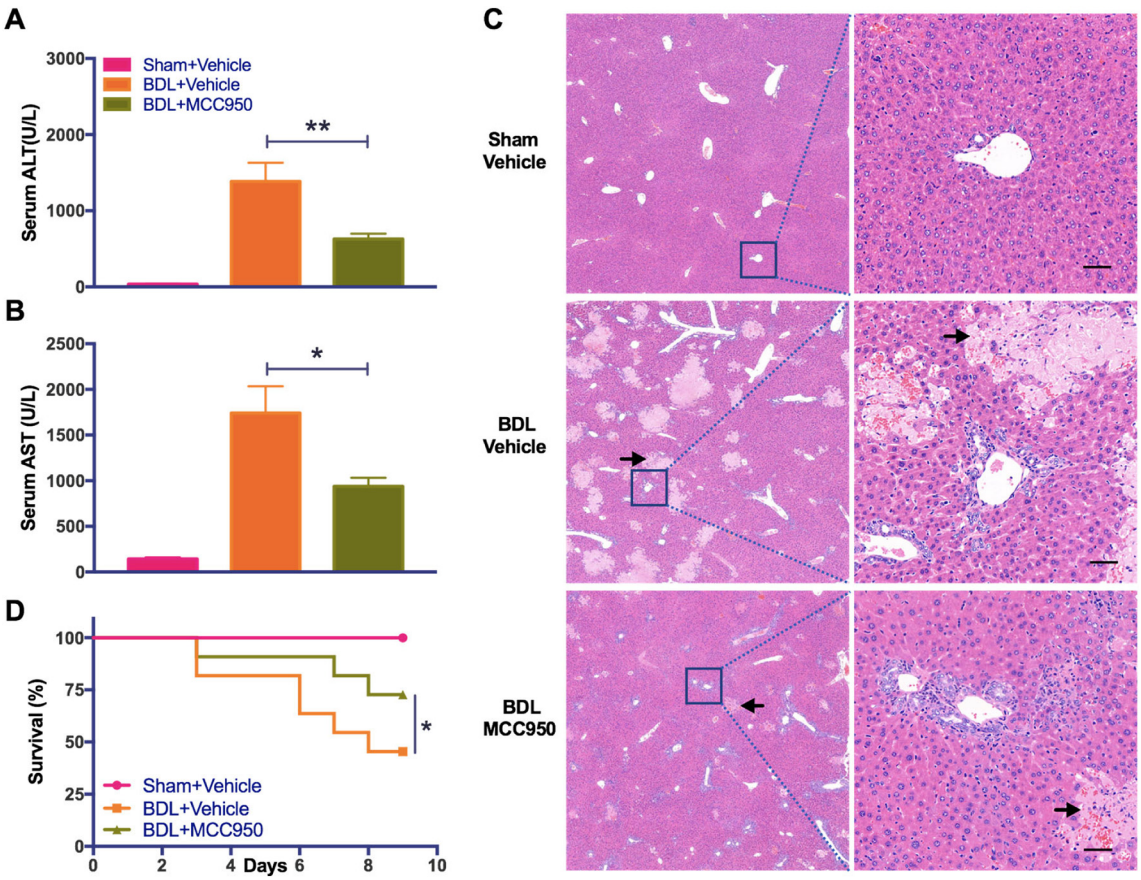

Fig. 1. MCC950 protects against BDL-induced liver injury and improves survival in mice. (A, B) Serum ALT and AST levels were significantly decreased in BDL + MCC950 mice compared to BDL mice. Data were expressed as means ± SEM (n = 5–7 per group). *P < 0.05, **P < 0.01 as compared with the BDL group. (C) Representative H&E stained liver sections that demonstrated focal necrosis in BDL mice livers are attenuated by MCC950. Scale bar = 50 μm. Black arrows show necrotic areas. (D) The Kaplan-Meier method was used to determine the difference in survival rate among the three groups. *P < 0.05 as compared with the BDL group using the log rank test.

3. Results

3.1. MCC950 attenuates liver injury and improves survival in BDL mice

To determine whether MCC950 has a protective role in cholestatic liver injury, MCC950 was administrated to mice at 10 mg/kg every day following bile duct ligation. As shown in Fig. 1A and B, the marked elevation of hepatocellular damage markers serum ALT and AST levels were notable in BDL mice, and MCC950 treatment reversed the cholestasis-induced increase in both markers. Notably, histopathology evaluation by H&E staining of the livers confirmed the biochemical results (Fig. 1C). Local coagulative necrosis, inflammatory cell infiltration, and bile duct proliferation reaction were markedly induced in the BDL group. On the other hand, liver specimens from the BDL + MCC950 group showed a clear limitation of hepatic injury. In addition, MCC950 treatment significantly increased the survival rate of BDL mice. The BDL mice had a survival rate of 45%. In contrast, the survival rate of the BDL + MCC950 group was 73% (Fig. 1D).

3.2. MCC950 retards development of BDL-induced liver fibrosis in mice

To determine the effect of MCC950 on BDL-induced hepatic fibrogenesis, histological examination of the liver sections was performed by staining with Sirius Red. As expected, the BDL mice showed increased collagen deposition via the Sirius Red staining (Fig. 2A), and an abnormality in histological collagen deposition was improved in the MCC950 group. Meanwhile, the alpha-smooth muscle actin (α-SMA) expression, a unique marker for activated hepatic stellate cells (HSCs), was analyzed by immunohistochemical staining. The results revealed the expression of α-SMA was gradually downregulated in BDL + MCC950 (Fig. 2B). Furthermore, RT-PCR was performed to analyze transforming growth factor β1 (TGF-β1), α-SMA, and Col1a1 compared to the sham group. Treatment with MCC950 appeared to significantly reduce hepatic expression of the aforementioned pro-fibrotic markers (Fig. 2C–E). These results suggest that MCC950 inhibits BDL-induced liver fibrosis in mice.

3.3. MCC950 decreases neutrophil infiltration and hepatic cell death during cholestatic liver injury

To further study the anti-inflammatory effect of MCC950 in cholestatic liver injury, neutrophil infiltration and cell death in liver tissues were examined. Results of immunohistochemical staining of myeloperoxidase (MPO), F4/80 (Fig. 3A-B), relevant mRNA transcripts for MPO (Fig. 3C), and infiltrating macrophages (Ly6c mRNA) (Fig. 3D) indicated hepatic inflammatory cell infiltration in BDL mice. However, BDL-induced hepatic inflammatory cell activation was attenuated by MCC950. Consistent with its effect on neutrophil infiltration, the TUNEL assay indicated the number of TUNEL-positive cells in BDL mice decreased after MCC950 administration (Fig. 3E). These data indicated that neutrophil infiltration and cell death during cholestatic liver injury were suppressed by MCC950.

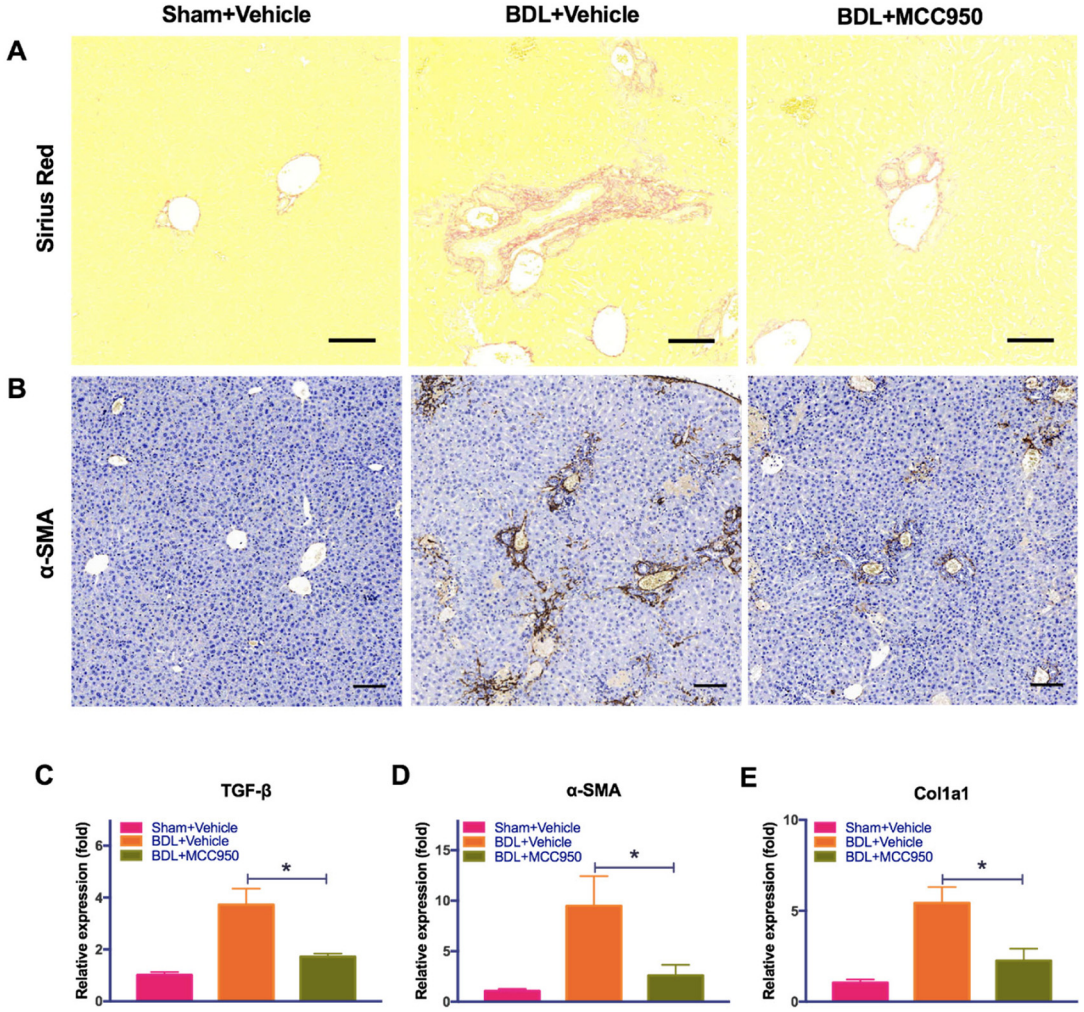

Fig. 2. MCC950 attenuated BDL-induced liver fibrosis. (A) Representative Sirius Red-stained liver sections. Scale bar = 100 μm. (B) Representative liver sections stained by α-SMA, scale bar = 100 μm. (C, D, E) The mRNA expression of TGF-β1, α-SMA and Col1a1 were detected by real-time PCR, normalized by β-actin and expressed as $2^{\Delta\Delta CT}$. Data were expressed as means ± SEM (n = 5–7 per group).*P < 0.05 as compared with the BDL group. (For interpretation of the references to color in this figure legend, the reader is referred to the web version of this article.)

3.4. MCC950 ameliorates NLRP3 inflammasome activation during cholestatic liver injury

To determine the effect mechanism of MCC950, the serum levels of pro-inflammatory cytokines using ELISA were examined. As shown in Fig. 4A and B, MCC950 application effectively decreased the elevated IL-1β and IL-18 levels caused by cholestasis. Moreover, the expression of NLRP3 inflammasome components were measured. Both the protein and mRNA levels of NLRP3, caspase-1 and IL-1β increased significantly after BDL compared with the sham operation, and the BDL + MCC950 group reversed this increase (Fig. 5A–D). In addition, NLRP3 expression in situ in mice liver tissue was also detected using IHC, and, as suspected, NLRP3-positive staining was increased in the periportal and portal areas of BDL mice. MCC950 apparently reduced NLRP3-positive cells in the BDL + MCC950 group. Taken together, these results demonstrate that MCC950 efficiently suppresses cholestasis-induced NLRP3 inflammasome activation.

3.5. Mechanisms underlying the effect of MCC950 by GO and KEGG analyses

To further explore the possible mechanism of MCC950 in cholestatic liver diseases, transcriptome analysis of liver tissue was performed in the BDL and BDL + MCC950 groups. In this study, DEGs were screened with |log2 fold change| > 1 and a *P*-value < 0.05. In total, 253 genes were differentially expressed. Of these, 97 genes were down-regulated and 156 were up-regulated in the liver tissues of the MCC950-treated group. The details are described in the Supplementary Table 2. To gain more insight into how MCC950 contributes to the protective effects of cholestatic liver injury we focused on the down-regulated genes, and GO and KEGG analyses were performed to explore the mechanisms. The GO analysis indicated the differentially expressed genes were associated with immune and inflammatory responses such as cytokine-mediated signaling pathways, regulation of defense response, inflammatory response, response to interferon-gamma, leukocyte differentiation, myeloid leukocyte activation, leukocyte cell-cell adhesion, negative regulation of immune system processes, leukocyte migration, I-kappa B kinase/NF-kappa B signaling, etc. (Fig. 6A). Meanwhile, the KEGG database was used to further understand the biological functions and pathways of the DEGs. The results indicated that a Toll-like receptor signaling pathway, chemokine signaling pathway, cytokine-cytokine receptor interaction, and NOD-like receptor signaling pathway may be involved in the pathogenesis of cholestatic liver injury (Fig. 6B). It was recognized the activation of innate immunity and liver inflammation will aggravate liver injury, therefore these pathways were chosen for further analysis.

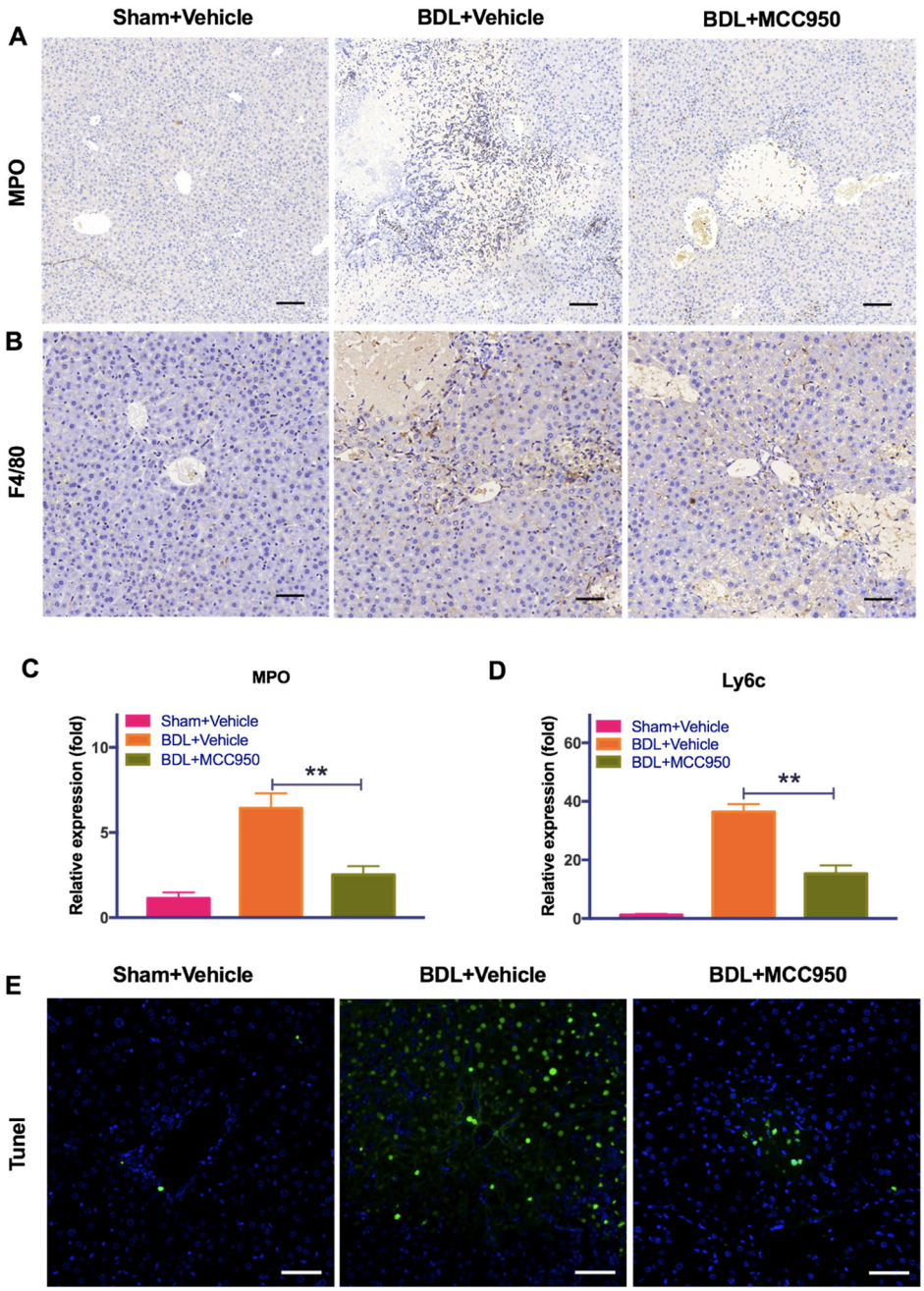

Fig. 3. MCC950 suppressed BDL-induced neutrophil infiltration and hepatocellular apoptosis. (A,B) Representative liver sections stained by MPO and F4/80. Scale bar = 100 μm. (C, D) The mRNA expression of MPO and Ly6c was determined by real-time PCR, normalized by β-actin, and expressed as $2^{\Delta\Delta CT}$. Data were expressed as means ± SEM (n = 5–7 per group). **P < 0.01 as compared with the BDL group. (E) Detection of hepatic apoptosis via a TUNEL assay and representative TUNEL positive staining in the liver sections. Scale bar = 100 μm.

3.6. Quantitative RT-PCR validation of the dysregulated genes involved in the inflammation related pathway

Results of the RNA sequencing experiments concerning the inflammation related pathway were further validated. Representative dysregulated genes, namely CD14, CXCL10, CCL5, STAT1, TLR2, IKBKE, TLR9, LIPG and SOCS1 in mRNA expression profiling results were selected for qRT-PCR validation. Consistent with the RNA sequencing data, the mRNA levels confirmed the expression levels of CD14, CXCL10, CCL5, STAT1, TLR2, and IKBKE in the liver tissue of the BDL + MCC950 group were significantly lower compared with the BDL group (Fig. 7A). TLR9, SOCS1 and LIPG was associated with a non-significant trend toward a decreased mRNA expression in BDL + MCC950 group as compared with BDL group (Fig. 7B).

4. Discussion

Cholestasis is characterized by the excessive accumulation of bile acids in hepatic tissue which can result in cholestatic liver injury, hepatic fibrosis, and cirrhosis [2,3]. The pathophysiology and mechanism of cholestasis is still undetermined and current therapy also has its limitations [18]. Thus, it is imperative to pursuit a new therapy. In this study, we aim to investigate the therapeutic effect and molecular mechanism of MCC950 against cholestatic liver injury and hepatic fibrosis induced by bile duct obstruction in mice.

Increasing evidence demonstrates NLRP3 inflammasome has been

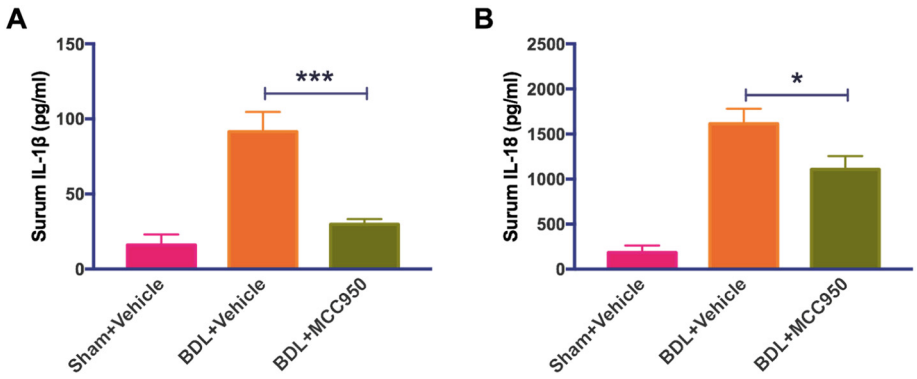

Fig. 4. MCC950 reduces inflammasome-associated pro-inflammatory cytokine levels during cholestatic liver injury. The serum was collected and cytokine levels were measured using an ELISA kit to determine the expression of IL-1β (A) and IL-18 (B). Data were expressed as means ± SEM (n = 5–7 per group). *P < 0.05, ***P < 0.001 as compared with the BDL group.

linked to various liver diseases. However, the role of NLRP3 in the development of cholestatic liver injury is still not clear. The current study has taken into consideration NLRP3 inflammasome in the pathogenesis of common bile duct ligation in mice, which are used widely as a cholestasis model. Our data show that bile duct obstruction markedly increased the expression of NLRP3 and its essential components (caspase-1, IL-1β) in BDL mice, suggesting the NLRP3 inflammasome pathway played an important role in response to obstructive liver injury. During cholestasis, bile acid-induced cell death can release damage-associated molecular patterns (DAMPs) and trigger a sterile inflammatory response in cholestasis [19]. Activated NLRP3 inflammasome induces the release of active caspase-1 from its

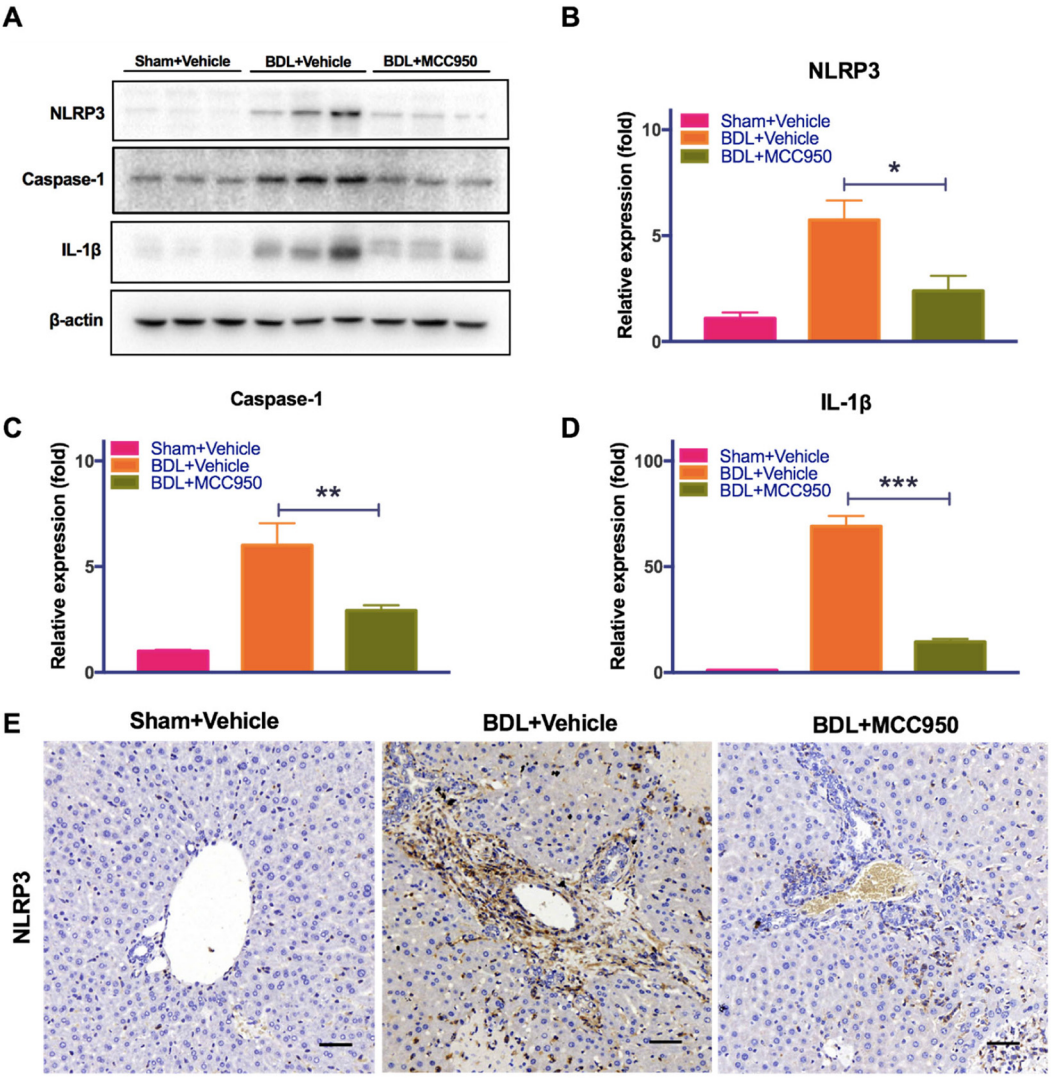

Fig. 5. MCC950 inhibited NLRP3 inflammasome activation during cholestatic liver injury. (A) The protein expression of NLRP3, cleaved caspase-1, and IL-1β in the livers were detected by western blot analysis. β-Actin served as a control. (B, C, D) The mRNA expression of NLRP3, caspase-1, and IL-1β were detected by real-time PCR, normalized by β-actin and expressed as $2^{-\Delta\Delta CT}$. Data were expressed as means ± SEM (n = 5–7 per group). *P < 0.05, **P < 0.01, ***P < 0.001 as compared with the BDL group. (E) Representative immunohistochemistry staining of NLRP3 in the liver tissues. Scale bar = 100 μm.

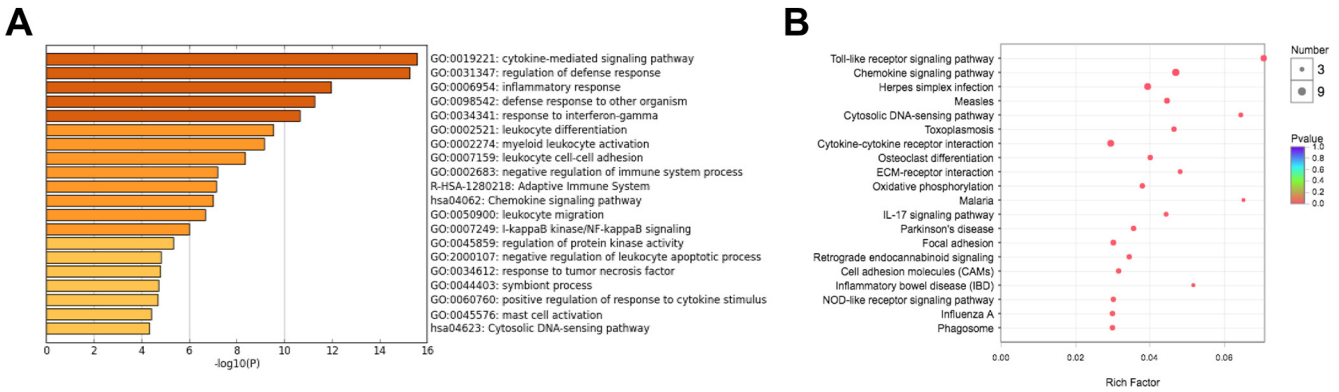

Fig. 6. (A) GO analysis predicted the function of differentially expressed genes. (B) KEGG analysis indicated the key signaling pathway correlated with differentially expressed genes.

precursor, which in turn stimulates the release of mature IL-1β and IL-18 from its precursor. These inflammatory cytokines are crucial mediators of liver injury. Previous studies have shown that MCC950 have potential anti-inflammatory effects in multiple systems. In the present study, MCC950 markedly decreases the level of serum ALT and AST, alleviating histological damage in BDL mice. Moreover, as shown earlier and confirmed in our study, MCC950 could inhibit inflammatory responses by down-regulating the expression of NLRP3, decreasing the neutrophil infiltration and downstream inflammatory cytokine release [13,20,21].

Neutrophils are one of the components of the liver's innate immune system. Neutrophils play a crucial role in the immediate response to pathogens as well as in sterile inflammation, and respond to DAMP released by damaged cells [22]. Recruitment of neutrophils contributes to liver injury during obstructive cholestasis [23]. In this study, we confirmed the activation of neutrophils during obstructive liver injury

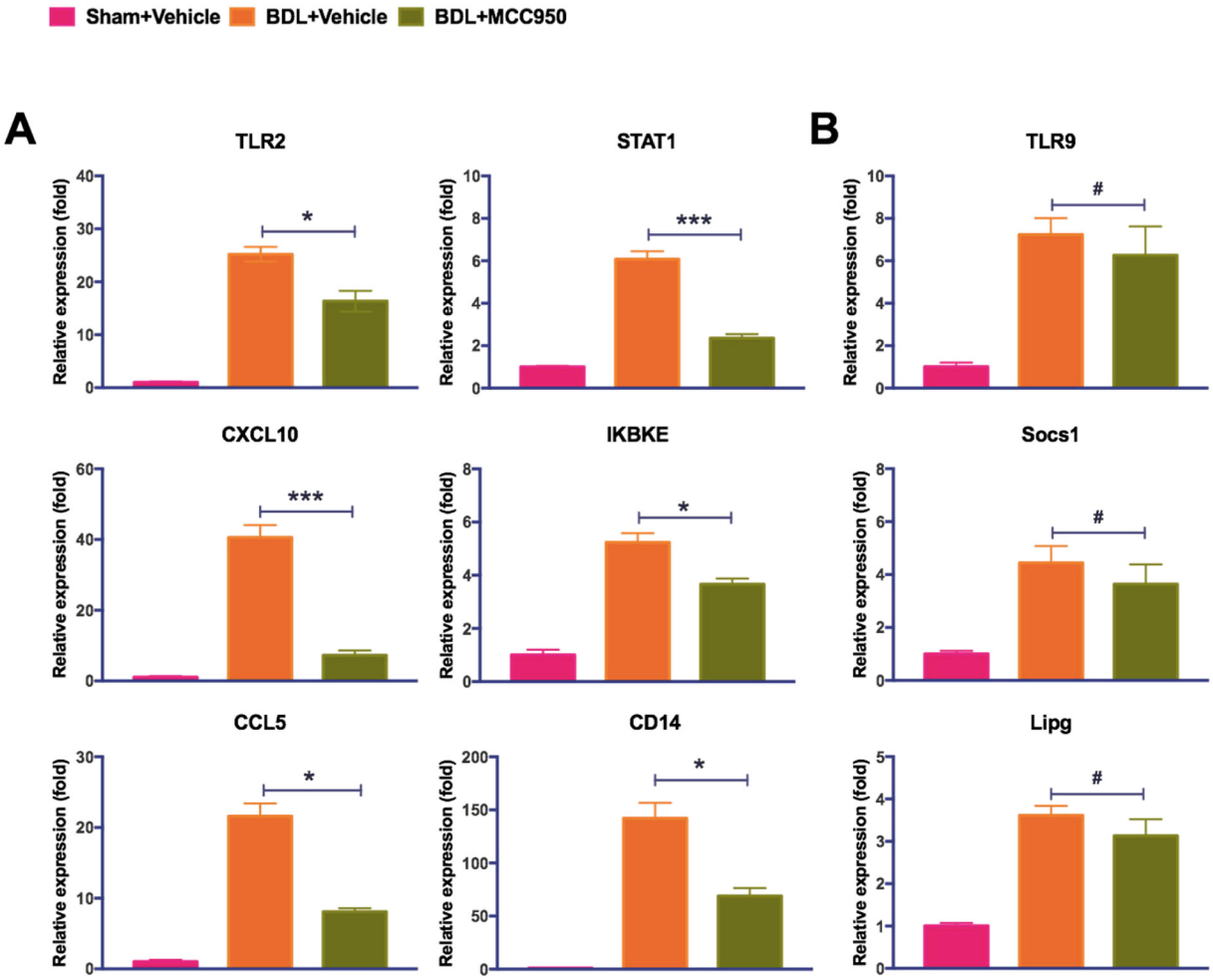

Fig. 7. Quantitative RT-PCR validation of the selected dysregulated genes. (A, B) The mRNA expression of CD14, CXCL10, CCL5, STAT1, TLR2, IKBKE, TLR9, SOCS1 and LIPG were detected by real-time PCR, normalized by β-actin and expressed as $2^{\Delta\Delta CT}$. Data were expressed as means ± SEM. *P < 0.05, ***P < 0.001, #P > 0.05 as compared with the BDL group (n = 5–7 per group).

and that NLRP3 inflammasome inhibition reduced neutrophil infiltration into the liver. We believe the limited neutrophil infiltration after MCC950 treatment may be attributed to the inhibition of the inflammasome-related IL-1β production, because IL-1β is critical for the promotion of inflammatory cells from the circulation into the extravascular [24]. In addition, inflammasome activation can induce programmed cell death (pyroptosis) [25]. In this study, we found an increase in TUNEL-positive hepatocytes in the BDL group indicating those hepatocytes undergo cell death. However, NLRP3 blocked mice with MCC950 were protected from this increase in TUNEL-positive cells. We hypothesize that a subset of cell death during cholestasis may be pyroptosis. Thus, we believe the protective effect of MCC950 during cholestasis may be partially attributed to attenuation of BDL-induced pyroptosis. Together, these data provide compelling evidence that MCC950 has a potential protective effect in cholestatic liver injury.

Liver fibrosis is a pathogenic result of persistent liver injury. The central feature of fibrosis is the increased production and deposition of extracellular matrix [26]. Growing evidence supports that inflammasome and its downstream effectors contribute to the progression of liver fibrosis [5,27,28]. Inflammasome components such as IL-1β can promote the proliferation and transdifferentiation of HSCs [29,30]. This induces the upregulation of fibrotic markers resulting in their activation, which leads to liver fibrosis. Furthermore, NLRP3 gene-deletion and pharmacological modulation were associated with protection against liver fibrosis [5,13,31,32]. In the present study, the results of histological examination of hepatic collagen and elevated expression of TGF-β1, α-SMA, and Col1a1 mRNA in the BDL group were suppressed in the BDL + MCC950 group. This indicated that MCC950 affords substantial protection against hepatic fibrosis in BDL mice.

Bile acid induced inflammatory response is a novel pathophysiologic mechanism of cholestatic liver injury [33,34]. Toll-like receptors (TLRs) are pattern recognition signal receptors that can be activated by cell damage prompted endogenous molecules, referred to as DAMP [35], and play a critical role in tissue damage initiated inflammatory responses [36]. Meanwhile, prior studies demonstrated that TLR2 stimulates the activation of inflammasome signaling [37] and contributes to liver damage in obstructive cholestasis [38]. Furthermore, previous research has suggested a molecular crosstalk between the TLR2 cascade and the NLRP3 inflammasome inducing a synergistic effect to inflammation [39]. In this study, we found the expressions of some genes associated with Toll-like receptor signaling pathway, such as TLR2, CD14, CXCL10, CCL5, STAT1, and IKBKE, were significantly up-regulated in liver tissue in the BDL group. and MCC950 treatment reversed the up-regulation. This suggests that Toll-like receptor signaling may be involved in the protective effects of MCC950 in cholestatic liver injury.

In summary, NLRP3 inflammasome was activated in the bile duct ligation mice. The selective NLRP3 inhibitor MCC950 treatment attenuated cholestatic liver injury and liver fibrosis, suggesting that mitigating NLRP3 inflammasome with a small molecule chemical inhibitor might have superior beneficial effects in the therapeutic strategy for cholestatic liver injury.

Supplementary data to this article can be found online at https://doi.org/10.1016/j.intimp.2019.02.016.

Disclosure of interest

No conflict of interest.

Acknowledgements

This work was supported by the National Natural Science Foundation of China (81600491).

References

[1] R. Poupon, O. Chazouilleres, R.E. Poupon, Chronic cholestatic diseases, J. Hepatol. 32 (2000) 129–140.
[2] G.M. Hirschfield, E.J. Heathcote, M.E. Gershwin, Pathogenesis of cholestatic liver disease and therapeutic approaches, Gastroenterology 139 (2010) 1481–1496.
[3] W.R. Kim, J. Ludwig, K.D. Lindor, Variant forms of cholestatic diseases involving small bile ducts in adults, Am. J. Gastroenterol. 95 (2000) 1130–1138.
[4] G. Szabo, T. Csak, Inflammasomes in liver diseases, J. Hepatol. 57 (2012) 642–654.
[5] A. Wree, A. Eguchi, M.D. McGeough, C.A. Pena, C.D. Johnson, A. Canbay, et al., NLRP3 inflammasome activation results in hepatocyte pyroptosis, liver inflammation, and fibrosis in mice, Hepatology 59 (2014) 898–910.
[6] X. Wu, L. Dong, X. Lin, J. Li, Relevance of the NLRP3 inflammasome in the pathogenesis of chronic liver disease, Front. Immunol. 8 (2017) 1728.
[7] L. Yang, T. Mizuochi, P. Shivakumar, R. Mourya, Z. Luo, S. Gutta, et al., Regulation of epithelial injury and bile duct obstruction by NLRP3, IL-1R1 in experimental biliary atresia, J. Hepatol. 69 (2018) 1136–1144.
[8] R.C. Coll, A.A. Robertson, J.J. Chae, S.C. Higgins, R. Munoz-Planillo, M.C. Inserra, et al., A small-molecule inhibitor of the NLRP3 inflammasome for the treatment of inflammatory diseases, Nat. Med. 21 (2015) 248–255.
[9] K.-Y. Xu, C.-Y. Wu, S. Tong, P. Xiong, S.-H. Wang, The selective Nlrp3 inflammasome inhibitor Mcc950 attenuates lung ischemia-reperfusion injury, Biochem. Biophys. Res. Commun. 503 (2018) 3031–3037.
[10] A.P. Perera, R. Fernando, T. Shinde, R. Gundamaraju, B. Southam, S.S. Sohal, et al., MCC950, a specific small molecule inhibitor of NLRP3 inflammasome attenuates colonic inflammation in spontaneous colitis mice, Sci. Rep. 8 (2018) 8618.
[11] G.P. van Hout, L. Bosch, G.H. Ellenbroek, J.J. de Haan, W.W. van Solinge, M.A. Cooper, et al., The selective NLRP3-inflammasome inhibitor MCC950 reduces infarct size and preserves cardiac function in a pig model of myocardial infarction, Eur. Heart J. 38 (2017) 828–836.
[12] Y. Yu, Y. Cheng, Q. Pan, Y.J. Zhang, D.G. Jia, Y.F. Liu, Effect of the selective NLRP3 inflammasome inhibitor mcc950 on transplantation outcome in a pig liver transplantation model with organs from donors after cardiac death preserved by hypothermic machine perfusion, Transplantation 103 (2) (2019) 353–362.
[13] A.R. Mridha, A. Wree, A.A.B. Robertson, M.M. Yeh, C.D. Johnson, D.M. Van Rooyen, et al., NLRP3 inflammasome blockade reduces liver inflammation and fibrosis in experimental NASH in mice, J. Hepatol. 66 (2017) 1037–1046.
[14] C.G. Tag, S. Sauer-Lehnen, S. Weiskirchen, E. Borkham-Kamphorst, R.H. Tolba, F. Tacke, et al., Bile duct ligation in mice: induction of inflammatory liver injury and fibrosis by obstructive cholestasis, J. Vis. Exp. 96 (2015) 52438.
[15] C. Trapnell, L. Pachter, S.L. Salzberg, TopHat: discovering splice junctions with RNA-Seq, Bioinformatics 25 (2009) 1105–1111.
[16] S. Tripathi, M.O. Pohl, Y. Zhou, A. Rodriguez-Frandsen, G. Wang, D.A. Stein, et al., Meta- and orthogonal integration of influenza "OMICs" data defines a role for UBR4 in virus budding, Cell Host Microbe 18 (2015) 723–735.
[17] C. Xie, X. Mao, J. Huang, Y. Ding, J. Wu, S. Dong, et al., KOBAS 2.0: a web server for annotation and identification of enriched pathways and diseases, Nucleic Acids Res. 39 (2011) W316–W322.
[18] Z. Yuan, G. Wang, J. Qu, X. Wang, K. Li, 9-cis-retinoic acid elevates MRP3 expression by inhibiting sumoylation of RXRalpha to alleviate cholestatic liver injury, Biochem. Biophys. Res. Commun. 503 (2018) 188–194.
[19] B.L. Woolbright, K. Dorko, D.J. Antoine, J.I. Clarke, P. Gholami, F. Li, et al., Bile acid-induced necrosis in primary human hepatocytes and in patients with obstructive cholestasis, Toxicol. Appl. Pharmacol. 283 (2015) 168–177.
[20] Y. Zhai, X. Meng, T. Ye, W. Xie, G. Sun, X. Sun, Inhibiting the NLRP3 inflammasome activation with MCC950 ameliorates diabetic encephalopathy in db/db mice, Molecules 23 (2018).
[21] X. Zhang, J. Luan, W. Chen, J. Fan, Y. Nan, Y. Wang, et al., Mesoporous silica nanoparticles induced hepatotoxicity via NLRP3 inflammasome activation and caspase-1-dependent pyroptosis, Nanoscale 10 (2018) 9141–9152.
[22] M. Li, S.Y. Cai, J.L. Boyer, Mechanisms of bile acid mediated inflammation in the liver, Mol. Asp. Med. 56 (2017) 45–53.
[23] J.S. Gujral, A. Farhood, M.L. Bajt, H. Jaeschke, Neutrophils aggravate acute liver injury during obstructive cholestasis in bile duct-ligated mice, Hepatology 38 (2003) 355–363.
[24] C.A. Dinarello, Immunological and inflammatory functions of the interleukin-1 family, Annu. Rev. Immunol. 27 (2009) 519–550.
[25] T. Bergsbaken, S.L. Fink, B.T. Cookson, Pyroptosis: host cell death and inflammation, Nat. Rev. Microbiol. 7 (2009) 99–109.
[26] F. Alegre, P. Pelegrin, A.E. Feldstein, Inflammasomes in liver fibrosis, Semin. Liver Dis. 37 (2017) 119–127.
[27] S.G. Boaru, E. Borkham-Kamphorst, L. Tihaa, U. Haas, R. Weiskirchen, Expression analysis of inflammasomes in experimental models of inflammatory and fibrotic liver disease, J. Inflamm. 9 (2012) 49.
[28] R.P. Witek, W.C. Stone, F.G. Karaca, W.K. Syn, T.A. Pereira, K.M. Agboola, et al., Pan-caspase inhibitor VX-166 reduces fibrosis in an animal model of nonalcoholic steatohepatitis, Hepatology 50 (2009) 1421–1430.
[29] F.P. Reiter, R. Wimmer, L. Wottke, R. Artmann, J.M. Nagel, M.O. Carranza, et al., Role of interleukin-1 and its antagonism of hepatic stellate cell proliferation and liver fibrosis in the Abcb4(−/−) mouse model, World J. Hepatol. 8 (2016) 401–410.
[30] Z. Yaping, W. Ying, D. Luqin, T. Ning, A. Xuemei, Y. Xixian, Mechanism of interleukin-1beta-induced proliferation in rat hepatic stellate cells from different levels of signal transduction, APMIS 122 (2014) 392–398.
[31] A. Watanabe, M.A. Sohail, D.A. Gomes, A. Hashmi, J. Nagata, F.S. Sutterwala, et al., Inflammasome-mediated regulation of hepatic stellate cells, Am. J. Physiol. Gastrointest. Liver Physiol. 296 (2009) G1248–G1257.
[32] R.G. Gieling, K. Wallace, Y.P. Han, Interleukin-1 participates in the progression from liver injury to fibrosis, Am. J. Physiol. Gastrointest. Liver Physiol. 296 (2009)

G1324–G1331.
[33] D. Yu, S.Y. Cai, A. Mennone, P. Vig, J.L. Boyer, Cenicriviroc, a cytokine receptor antagonist, potentiates all-trans retinoic acid in reducing liver injury in cholestatic rodents, Liver Int. 38 (2018) 1128–1138.
[34] K. Allen, H. Jaeschke, B.L. Copple, Bile acids induce inflammatory genes in hepatocytes: a novel mechanism of inflammation during obstructive cholestasis, Am. J. Pathol. 178 (2011) 175–186.
[35] M.E. Bianchi, DAMPs, PAMPs and alarmins: all we need to know about danger, J. Leukoc. Biol. 81 (2007) 1–5.
[36] T. Kawai, S. Akira, TLR signaling, Semin. Immunol. 19 (2007) 24–32.
[37] K. Miura, L. Yang, N. van Rooijen, D.A. Brenner, H. Ohnishi, E. Seki, Toll-like receptor 2 and palmitic acid cooperatively contribute to the development of non-alcoholic steatohepatitis through inflammasome activation in mice, Hepatology 57 (2013) 577–589.
[38] A. Ogawa, T. Tagawa, H. Nishimura, T. Yajima, T. Abe, T. Arai, et al., Toll-like receptors 2 and 4 are differentially involved in Fas dependent apoptosis in Peyer's patch and the liver at an early stage after bile duct ligation in mice, Gut 55 (2006) 105–113.
[39] Y. Naganuma, Y. Takakubo, T. Hirayama, Y. Tamaki, J. Pajarinen, K. Sasaki, et al., Lipoteichoic acid modulates inflammatory response in macrophages after phagocytosis of titanium particles through toll-like receptor 2 cascade and inflammasomes, J. Biomed. Mater. Res. A 104 (2016) 435–444.